ACSNANO
www.acsnano.org
ARTICLE

Elastin-like Polypeptide Linkers for Single-Molecule Force Spectroscopy

Wolfgang Ott,[†,‡,⊥] Markus A. Jobst,[†,⊥] Magnus S. Bauer,[†] Ellis Durner,[†] Lukas F. Milles,[†] Michael A. Nash,[§,∥] and Hermann E. Gaub*[,†]

[†]Lehrstuhl für Angewandte Physik and Center for NanoScience, Ludwig-Maximilians-Universität München, 80799 Munich, Germany
[‡]Center for Integrated Protein Science Munich (CIPSM), Ludwig-Maximilians-Universität München, 81377 Munich, Germany
[§]Department of Chemistry, University of Basel, 4056 Basel, Switzerland
[∥]Department of Biosystems Science and Engineering, Swiss Federal Institute of Technology (ETH Zurich), 4058 Basel, Switzerland

Supporting Information

ABSTRACT: Single-molecule force spectroscopy (SMFS) is by now well established as a standard technique in biophysics and mechanobiology. In recent years, the technique has benefitted greatly from new approaches to bioconjugation of proteins to surfaces. Indeed, optimized immobilization strategies for biomolecules and refined purification schemes are being steadily adapted and improved, which in turn has enhanced data quality. In many previously reported SMFS studies, poly(ethylene glycol) (PEG) was used to anchor molecules of interest to surfaces and/or cantilever tips. The limitation, however, is that PEG exhibits a well-known trans−trans−gauche to all-trans transition, which results in marked deviation from standard polymer elasticity models such as the worm-like chain, particularly at elevated forces. As a result, the assignment of unfolding events to protein domains based on their corresponding amino acid chain lengths is significantly obscured. Here, we provide a solution to this problem by implementing unstructured elastin-like polypeptides as linkers to replace PEG. We investigate the suitability of tailored elastin-like polypeptides linkers and perform direct comparisons to PEG, focusing on attributes that are critical for single-molecule force experiments such as linker length, monodispersity, and bioorthogonal conjugation tags. Our results demonstrate that by avoiding the ambiguous elastic response of mixed PEG/peptide systems and instead building the molecular mechanical systems with only a single bond type with uniform elastic properties, we improve data quality and facilitate data analysis and interpretation in force spectroscopy experiments. The use of all-peptide linkers allows alternative approaches for precisely defining elastic properties of proteins linked to surfaces.

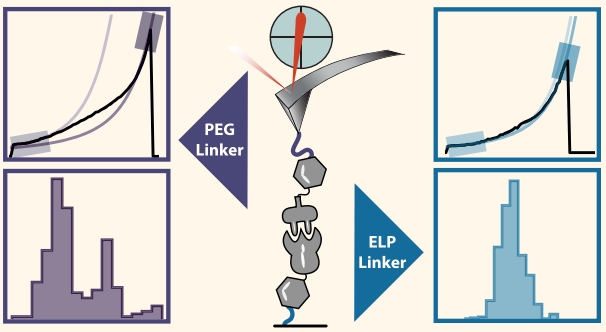

KEYWORDS: *single-molecule force spectroscopy, elastin-like polypeptides, biopolymer spacer, sortase coupling, protein ligation*

Refined Techniques in SMFS. Single-molecule force spectroscopy (SMFS) is a state-of-the-art technique in the rapidly growing field of molecular biomechanics.[1−3] Tools and methods are being steadily developed to improve ease of sample handling, sensitivity, reproducibility, and reliability.[4,5] In parallel, the biochemical toolbox is expanded continuously, enabling analysis of more complex and demanding biological systems. Improvements such as the use of orthogonal binding handles,[6−9] diverse biomolecule immobilization strategies,[10−14] and alternative methods for protein synthesis (*i.e.*, recombinant bulk expression or cell-free *in vitro* expression) are all examples of significant technical advances that have been achieved in recent years.[15]

Requirements for Recording Large Data Sets and Challenges Arising Therefrom. A key requirement to probe multiple different protein domains in a single experiment is the ability to use a single cantilever over extended periods of time to achieve a large number of force−extension traces. For this purpose, two main advances are worth noting, the first of them being the improvement of geometrically defined covalent surface tethering and the second being the discovery and characterization of the type III cohesin−dockerin (Coh:Doc) interaction.[7] Coh:Doc receptor−ligand pairs can withstand remarkably high forces in a SMFS assays and exhibit extremely high long-term functionality. This latter property is particularly important for carrying out multiplexed experiments where many proteins deposited onto the same surface and spatially

Received: April 18, 2017
Accepted: June 7, 2017
Published: June 7, 2017

DOI: 10.1021/acsnano.7b02694
ACS Nano XXXX, XXX, XXX−XXX

separated are pulled apart using the same receptor-modified cantilever. In such a configuration, Coh:Doc is used as a binding handle to successfully and continuously unfold target proteins for over 24 h of measurement time without significant loss of binding activity. Data sets of typically several tens of thousands of force−extension curves can easily be obtained using type III Coh:Doc, dramatically outperforming other mechanostable interactions (*e.g.*, biotin−avidin).

The ability to measure with a single cantilever over several days allows interrogation of different types or variants of proteins immobilized on different positions of the same substrate (*i.e.*, protein microarrays) and to achieve statistical significance over the course of a single experiment. This leads to large data sets and requires the use of sophisticated algorithms to identify and extract specific single-molecule interactions among a large number of traces with poor signal, such as empty traces, multiple interactions in parallel, or nonspecific interactions. Independent of the size of the data sets though, elasticity models whether applied as part of elaborate algorithms or fitted manually to single curves have in the past been required to account for the different elastic contributions stemming from heterogeneous stretching behavior of mixed poly(ethylene glycol) (PEG)−protein polymer backbone.

Conformational Changes of PEG Linker Molecules Obscure Molecular Characteristics of Interest. When performing SMFS in an elevated force regime using PEG as linker molecules, additional challenges arise. A conformational transition of PEG occurs in a force range of up to *ca*. 300 pN, resulting in an approximately linear force−extension regime.[16−18] In aqueous solutions, PEG exhibits a trans−trans−gauche conformation. With rising force on the polymer, the occupancy of conformations is shifted to all-trans, effectively increasing the net polymer contour length. Analysis methods such as fitting standard elasticity models to the data or detecting contour length increments within said force range are therefore compromised and would, for a quantitative description, require improved heterogeneous elasticity models.

PEG is a highly flexible polymer with a low persistence length, while peptide bonds have restricted degrees of freedom. These restrictions alter the stretching behavior and give rise to marked differences in comparison to PEG. Furthermore, the ratio of PEG linker length to unfolded protein backbone length is not constant over the course of an unfolding trace, which means fitting parameters must be optimized for different sections of the curve as more domains unfold. This issue becomes particularly significant and noticeable when probing protein unfolding and receptor−ligand unbinding in a high force regime and is also problematic when unfolding occurs across a broad range of forces.

Benefits of ELP Linkers in SMFS. In this study we investigate the feasibility of biological peptide polymers to circumvent this problem. We selected well-characterized elastin-like polypeptides (ELPs) as a suitable candidate for this purpose. The progression of cloning techniques of repetitive genes in recent years has set the stage for precisely defined protein polymers and opened up the ability to design, produce, and purify protein spacers of well-defined contour length and chemical composition for single-molecule experiments.[19−22] ELPs exhibit similar elasticity behavior as unfolded protein backbone and are completely monodisperse, a key advantage compared to synthetic polymers such as PEG. Monodisperse ELP linkers fused directly to a protein of interest allow for complete control of the lengths of a nanomechanical system from the surface up to the force transducer, which is not true for the chemically synthesized PEG polymers with non-negligible polydispersity. Since ELPs are expressed recombinantly in *Escherichia coli* (*E. coli*), their production is easily scaled up, resulting in lower costs compared to commercially available heterobifunctional PEGs. Furthermore, ELPs can be produced with N-/C-terminal protein ligation tags, which can be used for specific and bio-orthogonal surface chemistry in SMFS sample preparation.

ELPs are synthetic biopolymers derived from tropoelastin domains. They are composed of a repetitive amino acid heptamer "Val-Pro-Gly-Xaa-Gly",[23] where Xaa is a guest residue that can be any amino acid apart from proline. The guest residue influences the hydrophobicity of the protein and impacts the lower critical solution temperature, the point at which the ELP undergoes a soluble-to-insoluble phase transition. At this environment-dependent cloud point, ELPs change their conformation and precipitate, resulting in clouding of the solution.

ELPs are intrinsically disordered proteins that do not fold into well-defined secondary and tertiary structures, but rather remain unfolded and flexible, a property that is ideally suited to their application as spacer/linker molecules for SMFS.[24] We hypothesized that ELPs would therefore be a suitable choice to achieve both surface passivation and site-specific immobilization in single-molecule nanomechanical experiments. The bulky yet flexible features of ELPs inhibit nonspecific protein binding to the surface, while enabling ligation of other proteins due to the high degree of accessibility of N- or C-terminally fused peptide tags. Post-translational protein ligation methods have made it possible to move from organic chemical conjugation methods toward enzyme-mediated covalent immobilization, for example utilizing sortase A or Sfp.[14,25] Both enzymes catalyze sequence- and site-specific reactions yielding uniform protein orientation at the surface.

ELPs have previously been the subject of atomic force microscopy (AFM) studies. For example, AFM was used to support theoretical predictions about the behavior of ELPs above and below their cloud point, as well as to study ELP elasticity.[26−28] This study was carried out entirely below the cloud point, so that intermolecular interactions between ELPs were negligible. In contrast to prior studies, we employ ELPs as spacer molecules with other protein domains attached. Our results show that ELPs provide several benefits over PEG linkers in SMFS attributable primarily to the features of having uniform elastic properties and monodisperse linkers.

This study offers an attractive substitute for established PEG systems using all-protein ELP linkers. The immobilization strategy provides precise control over the elastic properties of multicomponent protein mechanical systems linked between a glass surface and a force transducer. Our approach transfers advances in smart polymer research to SMFS experiments and describes the improvements achieved through this alternative surface anchoring strategy.

RESULTS AND DISCUSSION

SMFS with Receptor−Ligand Polyproteins Employing Site-Specific Immobilization. Typically PEG linkers with an *N*-hydroxysuccinimide (NHS) group are linked to an aminosilanized surface. The other end of the PEG contains a reactive group for protein immobilization, which in most cases is a thiol-reactive maleimide group. Figure 1A illustrates a Coh:Doc-

DOI: 10.1021/acsnano.7b02694
ACS Nano XXXX, XXX, XXX−XXX

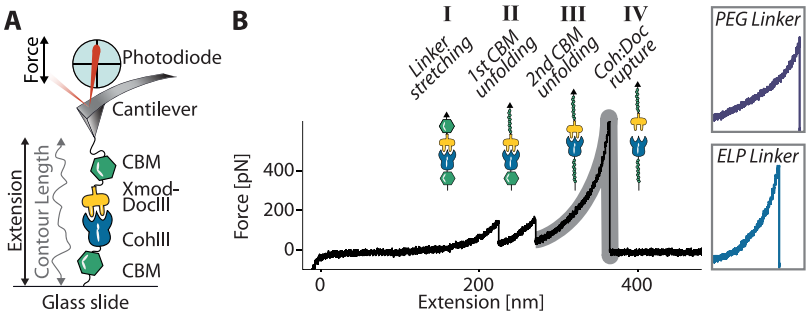

Figure 1. (A) SMFS configuration: Cantilevers are functionalized with CBM-Xmod-DocIII fusion proteins. Glass slides are modified with CohIII-CBM constructs. (B) Coh:Doc-based SMFS unfolding trace. Following Coh:Doc complex formation at zero extension, retraction of the cantilever results in mechanical stretching of the receptor:ligand-linked polyprotein. (I) Spacer molecules are fully extended and stretched. (II, III) The weakest links in the chain, usually the fingerprint domains (here: CBM), are unfolded in series. (IV) Finally, the Coh:Doc complex dissociates under force. The unfolded CBM domains can then refold after the complex rupture. The cantilever is now free to probe a different molecule on the surface. The insets on the right side qualitatively illustrate the differences in linker stretching in the high-force regime as observed in the final peak for constructs immobilized using PEG and ELP linkers. A quasi-linear regime of PEG stretching attributable to the conformational transition from trans-trans-gauche to all-trans is clearly visible for PEG in contrast to ELP.

based SMFS experiment. Proteins anchored to a functionalized glass surface are probed by the corresponding receptor fusion protein covalently linked to the cantilever tip. A characteristic unfolding curve recorded at constant speed is shown in Figure 1B. After the Coh:Doc complex is formed by contacting the cantilever with the surface, force is applied by retracting the base of the cantilever. The signal is detected by a quadrant photodiode with a laser that is reflected off the back side of the cantilever. Bending of the cantilever is translated into a differential voltage output of the photodiode. Upon retraction of the cantilever base at constant speed, the polymer linker is stretched first (Figure 1B, I). Subsequently, the weakest component in the system unfolds. In this case two carbohydrate binding modules (CBMs) are unfolded consecutively (Figure 1B, II and III). Finally, the force increases to a level where the receptor ligand pair dissociates. Following Coh:Doc rupture, the force drops to zero (Figure 1B, IV) and the cantilever is free to probe another molecule at a different location on the surface.

In order to identify data traces that show specific single-molecule interactions, a multilevel sorting algorithm is used to search for characteristic unfolding patterns of the fingerprint domains. This algorithm takes into account the unfolding forces and the measured increases in contour length (*i.e.*, contour length increments) of the peptide backbone upon unfolding of the various fingerprint domains.[29] Independent of the analysis method, however, accurate polymer elasticity models are required to quantify the hidden lengths of the folded proteins that are released by the unfolding events, giving rise to the limitations of PEG systems described above.

Adaptation of Surface Chemistry to Tether Protein Domains to ELP Linkers. The comparison of PEG with ELP linkers was carried out by cloning and recombinantly expressing two different ELPs both with 120 nm theoretical contour length ($ELP_{120\ nm}$, assuming 0.365 nm per amino acid).[30] One ELP linker contained an N-terminal sortase-tag ("GGG") and a C-terminal cysteine. The other ELP linker had a sortase-tag at its C-terminus ("LPETGG") and a cysteine at the N-terminus. Two analogous bioconjugation routes were used to attach ELP or PEG linkers to cantilevers and glass surfaces (Figure 2). To achieve a direct comparison, 15 kDa PEG linkers of similar contour lengths (~120 nm) were used. For PEG experiments, 15 kDa NHS-PEG-maleimide was immobilized onto an amino-silanized glass slide ($PEG_{120\ nm}$). The maleimide groups of the

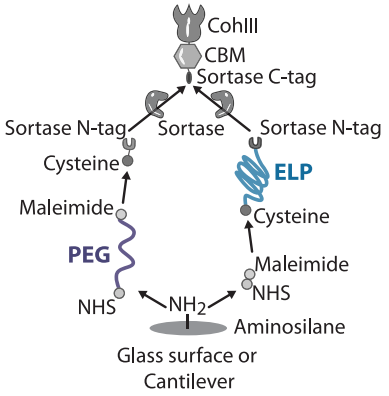

Figure 2. Comparison of immobilization strategies. For standard immobilization with PEG spacers, NHS chemistry was used to link PEG to amino-silanized surfaces. Protein constructs were then coupled *via* cysteine-sortase tag peptides to the maleimide end-groups on the PEG spacers. For immobilization with ELP linkers, a small-molecule NHS-maleimide cross-linker with a negligible contour length of 0.83 nm was used to couple cysteine-ELP spacers with a sortase-tag to the amino-silanized surface. In both cases, a fusion protein of interest, consisting of a CBM fingerprint domain and a mechanostable Coh receptor, was enzymatically coupled to the immobilized molecules on the surface in a subsequent step. Depicted is the functionalization of the glass surface with CohIII. The functionalization of the cantilever tip with DocIII followed a similar scheme.

PEG reacted with a GGGGG-Cys peptide, leaving the sortase N-tag available for subsequent derivatization. For ELP experiments, a small-molecule cross-linker (sulfosuccinimidyl 4-(*N*-maleimidomethyl)cyclohexane-1-carboxylate, sulfo-SMCC), which added negligible contour length (0.83 nm) to the system, was first immobilized onto amino-silanized glass, followed by coupling with GGG-$ELP_{120\ nm}$-Cys. Both strategies resulted in the sortase N-tag being available for conjugation *via* sortase-mediated enzymatic ligation. The protein of interest (CohIII-CBM-LPETGG) was linked by sortase A to ELP or PEG (Figure 2). The same strategy was used for the cantilever, except GGG-Xmod-DocIII was conjugated by sortase A to Cys-$ELP_{120\ nm}$-LPETGG or to $PEG_{120\ nm}$-coupled Cys-LPETGG. Our enzyme-mediated protein immobilization approach has the advantage of site-specific linkages and results in a homogeneous

DOI: 10.1021/acsnano.7b02694
ACS Nano XXXX, XXX, XXX−XXX

orientation of the proteins at the surface. Such uniformly immobilized proteins lead to a well-defined propagation of the applied force through the molecular complex under investigation and to well-defined distributions of the unfolding/rupture events in the force−extension curves. The use of N- and C-terminal tags for surface chemistry also ensured that only full-length (*i.e.*, fully translated) ELPs were measured in the experiment.

AFM experiments performed with ELPs as linkers showed a higher percentage of clearly identifiable single-molecule unfolding traces. We attribute this to the bulky character of the ELPs. They provide a less dense surface immobilization of the biomolecules of interest when compared to PEG-based immobilization. This behavior is advantageous since high surface density frequently causes multiple interactions between surface- and cantilever-bound molecules in SMFS experiments (Supplemental Figure S1). Multiple interactions are generated when more than one receptor−ligand interaction is formed in parallel. The complicated unfolding and unbinding traces that result from multiple bonds pulled in parallel are hardly interpretable and therefore discarded from the analysis (Supplemental Figure S2). Efficient passivation of glass surfaces against nonspecific adhesion of proteins requires a dense PEG surface layer, to prevent proteins from nonspecifically sticking to the glass surface. Approaches such as titrating functional (*i.e.*, maleimide end-groups) with nonfunctional (*i.e.*, CH_3 end-groups) PEG or changing the concentration of binding agents or proteins of interest can improve the process. In our experience, however, surface immobilization with ELP instead of PEG linkers leads to better passivation of the surface and a higher percentage of single-molecule traces without the need for any titration of functional and nonfunctional linkers.

Comparison of Dispersity between PEG and ELP Linkers. All unfolding traces were presorted by an automated analysis routine, selecting for single interactions that display two consecutive CBM unfolding events. Following the automated sorting, deletion of obviously erroneous curves (typically 10%) caused by, for example, baseline drift was performed manually.[7,29] PEG unfolding traces showed wildly varying initial extensions prior to the first CBM unfolding event. This is likely caused by the non-negligible polydispersity of PEG, as we did not observe multiple discrete populations with ELP experiments. The intrinsic monodispersity of ELP molecules is a clear advantage. Since they are produced recombinantly in *E. coli* with functional tags *in vivo*, only full-length protein sequences have the necessary terminal peptide tags that allow for surface immobilization. Additionally, ELPs were purified with inverse transition cycling (ITC), a method developed for ELP purification based on their reversible precipitation behavior. Possibly shorter ELPs are removed during the process, since their cloud point is higher than for $ELP_{120\ nm}$. Although the polydispersity of chemically synthesized PEGs (mass distribution ∼10−20 kDa) is sufficiently low for many applications, it leads to a noticeable impact in SMFS.

The influence of PEG polydispersity on the SMFS data is illustrated in Figure 3A, which shows SMFS traces recorded with both PEG and ELP linkers and also shows example traces of the shortest and largest extensions found in a typical type III Coh:Doc data set. Figure 3B shows a histogram of extension values at which the first CBM unfolding event occurred. For ELPs, the distribution shows one peak centered at an extension value that is expected based on the known ELP linker length. In the case of the PEG experiment, however, three distinct

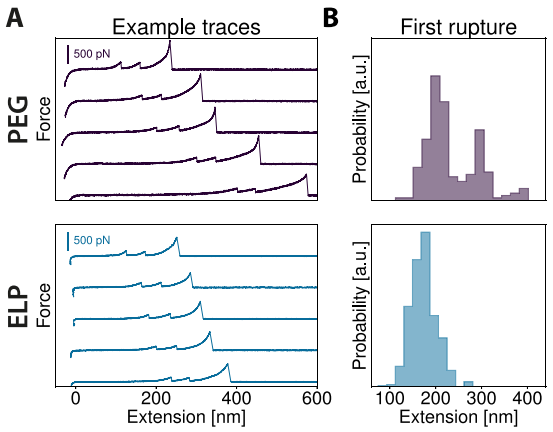

Figure 3. Comparison of dispersity of PEG and ELP linkers. (A) Typical force−extension traces for PEG (purple) and ELPs (blue). In the PEG linker experiment, the unfolding events occur over a wider range of absolute extension values, whereas unfolding events with ELP linkers occur over a narrow range. (B) Histograms showing the distribution of extension values corresponding to the first CBM unfolding event in each curve (PEG: N = 219; ELP: N = 521). Due to the polydispersity of the PEG linkers, three discrete populations with different extensions are clearly visible, while for ELPs only one population is observed.

populations are observed. This can be understood by considering that at the level of single molecules a polydisperse distribution results in discrete peaks representing the corresponding lengths of the discrete polymeric linkers on the cantilever tip. We interpret the distributions as being caused by three different PEG molecules with different lengths attached to the tip. Although the discrete distributions could conceivably be caused by different positions of the molecule attachment points to the AFM cantilever tip, this effect should be the same for ELPs. Moreover, varying linker lengths also reflect in varying steepness of the force−extension trace peaks, which would not occur simply because of attachment geometry (Figure 3A, PEG traces). We exclusively observed monomodal distributions for ELPs; therefore an anchor position effect seems not to play a major role. This polydispersity is clearly disadvantageous, since multiple linker lengths render data analysis more difficult. Curves cannot simply be overlaid in force−distance space due to varying loading rates. Furthermore, for constant-speed SMFS experiments, loading rate populations in dynamic force spectra will be broadened due to the probabilistic nature of the thermally driven rupture events.

We note that the PEG-modified surfaces are softer than ELP-modified surfaces during indentation of the tip into the polymer brush, as determined by the curvature at the beginning of each trace. The firmer ELP-modified surfaces require a lower indentation force to reach a linear force−distance regime after the initial soft indentation. For calibrating the inverse optical lever sensitivity, this is advantageous since high indentation forces can damage the molecules attached to the tip through adsorption and denaturation processes.[31]

Uniform ELP Stretching Behavior Minimizes Artifacts. We hypothesized that by replacing synthetic PEG linkers with biological ELP linkers, and thereby having a single type of polymer backbone throughout the mechanical system, better defined elasticity properties for the recording of force curves would be achievable. The persistence lengths of ELP peptide backbones should be comparable to those of unfolded protein

DOI: 10.1021/acsnano.7b02694
ACS Nano XXXX, XXX, XXX−XXX

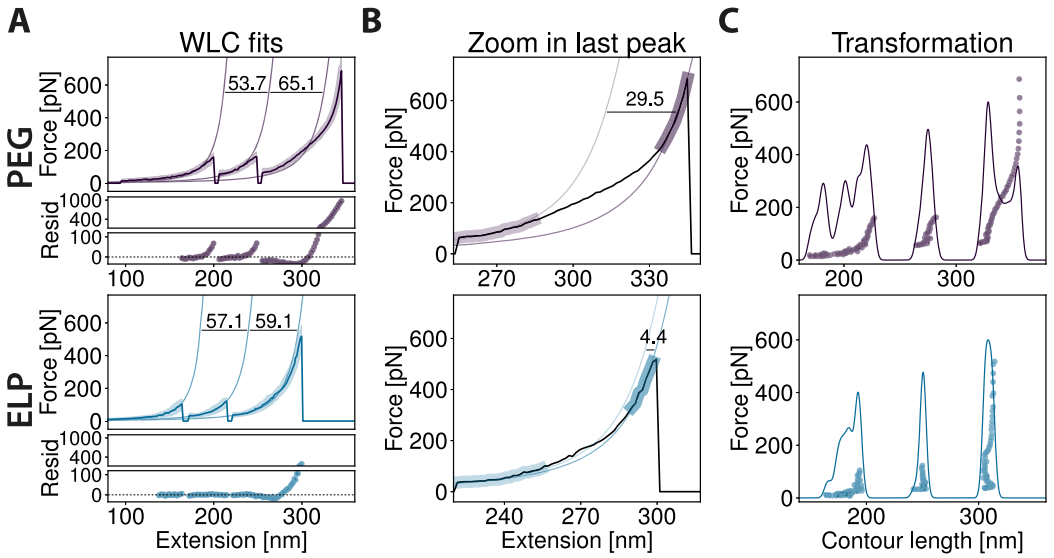

Figure 4. Elasticities of PEG and ELP linkers. (A) Superposition of multiple protein unfolding curves ("master curves") from SMFS experiments with PEG (purple, $N = 73$) and ELP linkers (blue, $N = 151$). The lower plots of each graph in panel A show the residuals of each WLC fit. Note that the residual plots are split into two subranges, shown in two windows from −35 to 120 pN (lower window) and from 120 to 1100 pN (upper window). The applied WLC model was extended by *ab initio* quantum mechanical calculations to correct for the enthalpic stretching of the polymer backbone.[33] Data were fitted with a fixed persistence length of 0.4 nm. The fits show that the stretching behavior of the mixed polymer system with PEG linkers deviates markedly at elevated forces from the predictions of the elasticity model, whereas the ELP curves agree reasonably well. (B) Final stretch and the Coh:Doc rupture event were fitted with the qmWLC model with two different contour lengths in the lower and upper force regime. The PEG molecules undergo a conformational transition,[16] resulting in different measured contour lengths for each force regime. For ELP molecules, a comparable transition was reported,[27,34] which apparently contributes to a much lower extent, so that SMFS experiments are much less affected. The differences in fitted contour length between the two fits are 29.5 nm for PEG linkers and 4.4 nm for ELP linkers. (C) Contour length transformations[29,35] of PEG and ELP master curves (purple and blue points). Ideally, the transformation results in data points aligning on vertical lines, where each line represents an energy barrier position for each stretching regime between two peaks in force−extension space. A KDE (Gaussian kernel, bandwidth: 2.5 nm) was calculated for the transformed data. The ELP data set showed the expected three peaks for the three unfolding and dissociation events, whereas the PEG data exhibit an irregular distribution with additional maxima.

domains, since they both consist of the same type of peptide-bonded polymer chains. This matching of the persistence length should be advantageous compared to PEG, which contains repeats of ethylene oxide groups with lower stiffness. Accurate description of the mechanical system under investigation by elasticity models plays a crucial role in determining characteristic parameters such as persistence lengths and contour length increments.

Previous studies had shown that at forces below 100 pN PEG elasticity may be satisfactorily described by standard elasticity models.[16] In a systematic study in this force range, we compared ELP and PEG linkers and corroborated these earlier results. The data and a thorough discussion thereof are given in the Supporting Information (see particularly Supplemental Figure S3).

At elevated forces, however, stretching of PEG through its conformational transition causes marked deviations from ideal polymer behavior. In aqueous environments, water molecules bridge neighboring ethylene oxide monomers by hydrogen bonding to two adjacent oxygen groups in the PEG backbone. By this means, water stabilizes the trans−trans−gauche configuration with a binding energy of around 3 kT. When PEG is stretched, however, the subunits of the backbone are forced increasingly into a slightly longer all-trans configuration and the bound water molecules are released. This conformational change, which contributes prominently to the polymer elasticity in the force range of up to ca. 300 pN, causes an increase in the measured net contour length of the polymer backbone.[16,17]

Figure 4A shows assemblies of multiple data traces ("master curves") of PEG- and ELP-linked proteins, respectively. The master curves are obtained by first aligning force−extension traces along the extension axis using an algorithm to maximize cross-correlation values in contour length space and then finding most probable force values of aligned traces in force distance space (see the Materials and Methods section). A recently introduced worm-like chain (WLC) approximation model[32] with an *ab initio* quantum mechanical correction for backbone stretching at high forces[33] (qmWLC) was then fitted to the traces with a fixed persistence length of 0.4 nm.

In the case of PEG linkers, a pronounced linear regime between 100 and 300 pN is visible in the last stretch prior to Coh:Doc rupture. As a consequence, the qmWLC cannot model this polymer correctly. ELPs do not show such a conformational change to this extent, and therefore the elasticity model fits satisfyingly. A fitting approach where the persistence length is also a free fit parameter is shown in Supplemental Figure S4. This approach misused the persistence length to compensate for the gauche-to-trans conformational change in the polymer; therefore, it resulted in largely unrealistic values for the contour length increments.

Figure 4B shows details of the last stretch before the Coh:Doc dissociation, highlighting the difference between PEG and ELP linkers. Two separate fits in the respective low- and high-force regimes illustrate the differences in polymer length before and after the conformational transition. We note that ELPs were also reported to have a force-induced conformational change, in this case based on proline cis−trans

DOI: 10.1021/acsnano.7b02694
ACS Nano XXXX, XXX, XXX−XXX

isomerization that also extends the contour length.[27,34] However, the low number of prolines in the overall sequence (every fifth amino acid) in the ELP motif renders this effect much smaller compared to the conformational change of PEG and will be camouflaged by signal noise in typical experiments with proteins.

Figure 4C shows the transformation into contour length space using the qmWLC model. A kernel density estimate (KDE) was used (Gaussian kernel, bandwidth of 2.5 nm) to generate smooth functions describing the contour length increments observed between unfolding or rupture events, which in this case included 2× CBM unfolding and Coh:Doc dissociation. In the case of PEG linkers, the KDE−contour length distribution shows several peaks. This is because of the failure of the qmWLC model to accurately describe the force response of the polymer. Determining the contour length increments between the peaks of the KDE proves problematic even for this relatively simple exemplary case of two large fingerprint unfolding events and a receptor ligand dissociation. Smaller unfolding steps or even folding intermediates, which appear as substeps, would be even harder to pinpoint with the PEG system. In the case of ELP-immobilized proteins, only three distinct peaks appear, with much more clearly identifiable contour length increments between the peaks.

CONCLUSION

PEG linkers have successfully been employed in numerous studies to anchor biomolecules of interest to surfaces for SMFS. In the low-force regime (below 100 pN) the extended WLC model describes their elastic properties with sufficient accuracy for the majority of applications. For elevated forces, however, the conformational transitions in the PEG backbone would necessitate further development of elasticity models for a convincing description.[16] Moreover, the inherent polydispersity of PEGs, together with their complex elasticity, complicates data analysis and reduces the amount of information that can be deduced from SMFS.

The ELP-based linkers, however, have proven in our studies to be significantly improved linker molecules for surface immobilization and passivation purposes in single-molecule force experiments. ELPs are monodisperse, are highly flexible, and readily allow for direct, site-specific tethering. We showed that these features lead to more accurate measurements of contour length increments in receptor−ligand polyprotein force spectroscopy experiments. A well-established elasticity model suffices for the data analysis.

Even at low forces, the PEG subunits already start to change their conformational state occupancy. At 50 pN, the probability for their elongated state is already above 10%.[16] Therefore, the findings we present here are also relevant for investigations at lower forces or in systems that should be analyzed over a large range of forces. PEG linkers may still deliver satisfying results, as long as data in similar force ranges can be compared. In some cases, elasticity parameters such as the Kuhn length or persistence length can heuristically compensate for effects not explicitly described by the model. As soon as different force ranges of multiple domains need to be compared, though, the varying proportions of elongated (all-trans) *versus* non-elongated (trans−trans−gauche) PEG subunits cannot simply be accounted for by the elasticity parameter, and therefore measured contour length increments get distorted. Different biochemical approaches like those described here are thus necessary to gain meaningful insights. These scenarios include, for example, shielded unfolding events or small substeps, where the force cannot drop sufficiently in between stretching events.

The ELPs investigated here represent only one formulation of the vast variety of smart polymer linkers that could be utilized in SMFS experiments. Further studies are required to evaluate other nonstructured, non-proline-containing protein linkers to determine their suitability for SMFS studies, since the amino acid side chain composition may affect the persistence length[36,37] or give rise to nonentropic behavior. Biotechnological characteristics, *i.e.*, recombinant production yields and ease of purification, are as important as the biophysical requirements, which renders the easily produced ELPs particularly attractive. Other smart polymers should be similarly accessible to perform as suitable alternatives. The reported approach can be applied to enhance SMFS studies with purified proteins on functionalized surfaces as shown here or alternatively to modify cantilevers for chemical recognition imaging and force spectroscopy on artificial membranes or cell surfaces. It can easily be adopted by standard molecular biology equipped laboratories to streamline the procedure and improve data quality for resolving smaller unfolding features with high accuracy. Studies on smart polymers as tethers for SMFS experiments might also help to develop environmentally responsive surfaces, which bear potential for exciting applications in the nanobiosciences.

MATERIALS AND METHODS

All reagents were at least of analytical purity grade and were purchased from Sigma-Aldrich (St. Louis, MO, USA) or Carl Roth GmbH (Karlsruhe, Germany). All buffers were filtered through a 0.2 μm poly(ether sulfone) membrane filter (Nalgene, Rochester, NY, USA) prior to use. The pH of all buffers was adjusted at room temperature.

A 300 amino acid long ELP was the basis for the AFM linker constructs used in this study, and the underlying cloning and protein purification procedure of the ELP is described in detail elsewhere.[19] The ELP sequence was $[(VPGVG)_5\text{-}(VPGAG)_2\text{-}(VPGGG)_3]_6$ and is referred to as $ELP_{120\ nm}$.

Standard molecular biology laboratories capable of producing recombinant proteins are equally capable of expressing ELPs, since both rely on the same principles, reagents, and instrumentation. With our plasmids provided at Addgene, cloning can even be avoided and production of ELP linkers for protein immobilization can be performed right away.

Cloning. A detailed description of the cloning procedure of the constructs can be found in the Supporting Information (Figures S5−S11). ELP sequences used in this study, along with 40 nm length variants and binding handles, are deposited at Addgene and available upon request (Addgene accession numbers: 90472: Cys-$ELP_{120\ nm}$-LPETGG, 90475: Cys-$ELP_{40\ nm}$-LPETGG, 91571: GGG-$ELP_{40\ nm}$-Cys, 91572: GGG-$ELP_{120\ nm}$-Cys, 91697: CohIII-CBM-HIS-LPETGG, 91698: GGG-HIS-CBM-Xmod-DocIII).

Transformation of Cells. A 2 μL amount of Gibson assembly or ligation reaction transformed *DH5α* cells (Life Technologies GmbH, Frankfurt, Germany; 30 min on ice, 1 min at 42 °C, 1 h at 37 °C in SOC medium) was used. The cells were plated on 50 μg/mL kanamycin-containing LB agar and incubated overnight at 37 °C. Clones were analyzed with Colony PCR, and clones with amplicons of appropriate lengths were sent to sequencing.

Protein Expression. Chemically competent *E. coli NiCo21(DE3)* (New England Biolabs, Ipswich, MA, USA) were transformed with 50 ng of plasmid DNA for the expression of all constructs used in this study. Transformed cells were incubated in autoinduction ZYM-5052 media (for ELP containing constructs supplemented with 5 mg/mL proline, valine, and 10 mg/mL glycine; 100 μg/mL kanamycin) for 24 h (6 h at 37 °C, 18 h at 25 °C).[38] Expression cultures were harvested *via* centrifugation (6500*g*, 15 min, 4 °C), the supernatant was discarded, and the pellets were stored at −80 °C until further lysis.

DOI: 10.1021/acsnano.7b02694
ACS Nano XXXX, XXX, XXX−XXX

Throughout the whole purification process, for ELPs containing a cysteine, 1 mM tris(2-carboxyethyl)phosphine (TCEP, Thermo Fisher Scientific Inc., Waltham, MA, USA) or 1 mM of dithiothreitol (DTT) was added to the respective buffers. Cell pellets with proteins containing no HIS-tag were solubilized in 50 mM Tris-HCl pH 7.5 (supplemented with cOmplete, EDTA-free protease inhibitor cocktail, Sigma-Aldrich, St. Louis, MO, USA), and all other pellets in lysis buffer (50 mM Tris, pH 8.0, 50 mM NaCl, 10% (w/v) glycerol, 0.1% (v/v) Triton X-100, 5 mM $MgCl_2$, DNase I 10 μg/mL, lysozyme 100 μg/mL).

Cys-$ELP_{120\ nm}$-LPETGG and GGG-$ELP_{120\ nm}$-Cys were purified with the ITC method.[39] After resolubilization, the cells were lysed by sonication (Bandelin Sonoplus GM 70, tip: Bandelin Sonoplus MS 73, Berlin, Germany; 40% power, 30% cycle, 2 × 10 min). The cells were kept on ice during the sonication procedure. The soluble fraction was separated from the insoluble cell debris by centrifugation (15000*g*, 4 °C, 1 h). In a first heating step (60 °C, 30 min) of the supernatant, most of the *E. coli* host proteins precipitated. The fraction of the collapsed ELPs was resolubilized by cooling the suspension for 2 h to 4 °C on a reaction tube roller. The insoluble host proteins were pelleted by centrifugation (15000*g*, 4 °C, 30 min). Further purification steps were necessary to increase the purity of the ELP solution. This was done by repeated thermoprecipitation of the ELP followed by redissolution.

The ELP solution was clouded by adding 1 M acetate buffer (final concentration 50 mM, pH 2.5) and 2 M NaCl. A heating step (60 °C, 30 min) ensured all ELPs were collapsed. A hot centrifugation (3220*g*, 40 °C, 75 min) was necessary to separate the high-salt, low-pH solution from the ELP pellet, which was resolubilized in 50 mM Tris-HCl (pH 7.0) after discarding the supernatant. The solution was incubated for 2 h at 4 °C to resolubilize all ELPs completely. A cold centrifugation step (3220*g*, 4 °C, 60 min) isolated the remaining insoluble fraction of the suspension. After decanting the supernatant, the salt concentration was increased and pH lowered, to precipitate the ELPs again. This cycle was repeated three times or extended if the purity of the solution was not high enough.

The constructs CohIII-CBM-HIS-LPETGG and GGG-HIS-CBM-Xmod-DocIII were expressed and lysed as described above. After the first centrifugation, the supernatant was, however, filtered (0.45 μm) and applied to a HisTrap FF (GE Healthcare Europe GmbH, Freiburg, Germany). Unspecifically bound proteins on the column were removed by washing five column volumes (25 mM Tris-HCl pH 7.8, 500 mM NaCl, 20 mM imidazole, Tween 20 0.25% (v/v), 10% (v/v) glycerol). Finally, the desired HIS-tag containing protein was eluted (25 mM Tris-HCl pH 7.8, 500 mM NaCl, 300 mM imidazole, Tween 20 0.25% (v/v), 10% (v/v) glycerol).

For long-term storage the protein solutions of the different constructs were concentrated (Amicon Ultra-15 centrifugal filter units 10K MWCO, Merck KGaA, Darmstadt, Germany) and reduced with 5 mM TCEP overnight (at 4 °C) for constructs that contained a cysteine. The buffer of the reduced ELP solution was exchanged (Zeba spin desalting columns 7K, Thermo Fisher Scientific Inc.) to 50 mM sodium phosphate, 50 mM NaCl, 10 mM EDTA, with a pH of 7.2, and 10% (v/v) glycerol and flash frozen in liquid nitrogen in small aliquots to be stored at −80 °C. All other proteins were exchanged with 25 mM Tris-HCl, 75 mM NaCl, and 5 mM $CaCl_2$ with a pH of 7.2 and supplemented with a final glycerol concentration of 20% (v/v). No loss of functionality of the ELPs (cross-linking and passivation capability) could be detected, when stored buffered or lyophilized in small aliquots at −80 °C, over the duration of more than one year.

SDS-PAGE (Any kD Mini-PROTEAN stain-free gels, Bio-Rad Laboratories GmbH, Hercules, CA, USA) was employed to detect any impurities. Since ELPs could not be stained with the stain-free technology, an Alexa Fluor 647-C_2-maleimide dye (Thermo Fisher Scientific Inc.) was incubated for 1 h at room temperature with the ELP solution. An appropriately diluted protein solution was mixed with 5× loading buffer (250 mM Tris-HCl, pH 8.0, 7.5% (w/v) SDS, 25% (v/v) glycerol, 0.25 mg/mL bromophenol blue, 12.5% (v/v) 2-mercaptoethanol) and heated for 5 min at 95 °C.

ELP concentration was photometrically determined at 205 nm (Ultrospec 3100 Pro, Amersham Biosciences, Amersham, England, and TrayCell, Hellma GmbH & Co. KG, Müllheim, Germany). For all other constructs an absorption measurement at 280 nm led to the concentration (NanoDrop UV−vis spectrophotometer, Thermo Fisher Scientific Inc.). The extinction coefficient was determined theoretically for ELPs at 205 nm[40] and 280 nm[41] for all other fusion proteins.

AFM Sample Preparation. Force spectroscopy samples, measurements, and data analysis were prepared and performed according to previously published protocols.[10,35] Silicon nitride cantilevers (Biolever mini, BL-AC40TS-C2, Olympus Corporation, Tokyo, Japan; nominal spring constant: 100 pN/nm; 25 kHz resonance frequency in water) were used as force probes. Surface chemistry for cantilevers was similar to that for coverslips (Menzel Gläser, Braunschweig, Germany; diameter 24 mm). Surfaces were amino-silanized with 3-(aminopropyl)dimethylethoxysilane (APDMES, ABCR GmbH, Karlsruhe, Germany). α-Maleinimidohexanoic-ω-NHS PEG (NHS-PEG-Mal, Rapp Polymere, Tübingen, Germany; PEG-MW: 15 kDa) was used as a linker for the sortase peptides (GGGGG-C and C-LPETGG, Centic Biotec, Heidelberg, Germany) in PEG-linked experiments. The cysteine-containing ELPs were linked to the surface with a sulfosuccinimidyl 4-(*N*-maleimidomethyl)cyclohexane-1-carboxylate) cross-linker (sulfo-SMCC, Thermo Fisher Scientific Inc.). PEG or cross-linker (10 mM) was dissolved in 50 mM 4-(2-hydroxyethyl)-1-piperazineethanesulfonic acid (HEPES) pH 7.5.

Sortase-catalyzed coupling of the fingerprint molecules (GGG-CBM-Xmod-DocIII and CohIII-CBM-LPETGG) was done in 25 mM Tris-HCl, pH 7.2, 5 mM $CaCl_2$, and 75 mM NaCl at 22 °C for 2 h. Typically, 50 μM ELP or sortase peptide was coupled with 25 μM fingerprint molecule and 2 μM sortase enzyme.

In between both of the cross-linking steps (PEG, SMCC, or ELP, peptide reaction) surfaces were rinsed with water and dried with nitrogen. After immobilization of the fingerprint molecules, surfaces were rinsed in measurement buffer (25 mM Tris-HCl, pH 7.2, 5 mM $CaCl_2$, 75 mM NaCl). The reaction of the different surface chemistry was done spatially separated by using silicone masks (CultureWell reusable gaskets, Grace Bio-Laboratories, Bend, OR, USA). The mask was applied after silanization and removed under buffer after the last immobilization step.

AFM-SMFS Measurements. Data were taken on custom-built instruments (MFP-3D AFM controller, Oxford Instruments Asylum Research, Inc., Santa Barbara, CA, USA; piezo nanopositioners: Physik Instrumente GmbH & Co. KG, Karlsruhe, Germany, or Attocube Systems AG, Munich, Germany).

Instrument control software was custom written in Igor Pro 6.3 (Wavemetrics Inc., Portland, OR, USA). Piezo position was controlled with a closed-loop feedback system running internally on the AFM controller field-programmable gate array. A typical AFM measurement took about 12 h and was done fully automated and at room temperature. Retraction velocity for constant-speed force spectroscopy measurements was 0.8 μm/s. Cantilever spring constants were calibrated after completing all measurements on different spots on the surface using the same cantilever. This was done by utilizing the thermal method applying the equipartition theorem to the one dimensionally oscillating lever.[31,42]

Force−Extension Data Analysis. Obtained data were analyzed with custom-written software in Python (Python Software Foundation, Python Language Reference, version 2.7, available at http://www.python.org), utilizing the libraries NumPy, SciPy, and Matplotlib.

Raw voltage data traces were transformed into force distance traces with their respective calibration values after determining the zero force value with the baseline position. A correction of the force-dependent cantilever tip *z*-position was carried out. Force distance traces were filtered for traces showing two CBM unfoldings and a subsequent type III cohesin−dockerin dissociation, without preceding Xmodule unfolding.[7] This screening was carried out by detecting maximum-to-maximum distances of kernel density estimate (Gaussian kernel, bandwidth 1 nm) peaks in contour length space in each single trace, after applying thresholds for force, distance, and number of peaks. For

DOI: 10.1021/acsnano.7b02694
ACS Nano XXXX, XXX, XXX−XXX

sorting data sets, transformation of force distance data into contour length space was done with a manually fixed persistence length of 0.4 nm, to measure distances of energy barrier positions.[29,43] Sorting was done allowing generous errors to the expected increments to account for the conformational stretching of the spacer molecules. Fits to the force−extension data with the WLC model had the following parameters additionally to the values mentioned in the figure captions, if not stated otherwise: initial guess for persistence length: 0.4 nm; fit precision: 1×10^{-7}. For assessment of transformation quality, the inverse worm-like-chain model was applied for transformation of force distance traces into the contour length space in a force window of 10 to 125 pN and with a persistence length previously fitted to each peak separately: The global mean value of each data set for each peak was used. Final alignments of the whole data sets were assembled by cross-correlation.

Master Curve Assembly. The master curves were assembled by cross-correlation of each force−distance trace of a presorted data set with all previous curves in contour length space, starting with a random curve. Each curve was shifted on its x axis to fit the maximum correlation value and added to the set assembly in contour length space. Subsequently, a second run was performed, cross-correlating each curve with the previously assembled set, to facilitate an equal correlation template for every curve, independent of its occurrence. Finally, the most probable shift was calculated by a KDE and subtracted from each curve to get representative absolute distances with respect to the origin. Distance and correlation value thresholds were applied to filter out less probable PEG populations and otherwise badly fitting data. In a final step, all overlaid raw data points in force−distance space were binned on the x axis into nanometer-sized slices, and their densities on the y axis were estimated by a KDE for each slice. Near the rupture events, where the kernel density estimates cannot unambiguously identify maxima of the data slices, the value was set to zero. Therefore, after each rupture, a small "gap" is visible, which was not included in data points used for fitting. Their most probable value and the corresponding full width at half-maxima then assembled the master curve. Although by this procedure representative absolute rupture forces for the domains are not necessarily reproduced to the highest accuracy, the most probable and most representative pathway of the elastic behavior in between peaks is resembled well.

qmWLC model. For WLC fits and transformations into contour length space, a recently improved approximation, solved for the extension, was used,[32] adding correction terms for quantum mechanical backbone stretching.[33]

With the abbreviations

$$f = FL_p/kT \tag{1}$$

$$b = \exp\left(\sqrt[4]{\frac{900}{f}}\right) \tag{2}$$

WLC fits were done with the model formula

$$x = L_{corr}\left(\frac{4}{3} - \frac{4}{3\sqrt{f+1}} - \frac{10b}{\sqrt{f}(b-1)^2} + \frac{f^{1.62}}{3.55 + 3.8f^{2.2}}\right) \tag{3}$$

With the quantum mechanical correction,

$$L_{corr} = \frac{L_{c,0}}{2y_2}\left(\sqrt{4Fy_2 + y_1^2} - y_1 + 2y_2\right) \tag{4}$$

where y_1 and y_2 are the *ab initio* parameters from the original publication.

Transformations were performed with the model contour length:

$$L_c = \frac{x}{\frac{4}{3} - \frac{4}{3\sqrt{f+1}} - \frac{10b}{\sqrt{f}(b-1)^2} + \frac{f^{1.62}}{3.55 + 3.8f^{2.2}}} \tag{5}$$

With the reverse quantum mechanical correction for zero force contour length,

$$L_{c,0} = \frac{L_c}{\frac{1}{2y_2}\left(\sqrt{y_1^2 + 4y_2F} + 2y_2 - y_1\right)} \tag{6}$$

with x being the extension, L_c the model contour length, F the force, L_p the persistence length, k Boltzmann's constant, T the temperature, y_1 and y_2 the quantum mechanical correction parameters, L_{corr} the qm-corrected contour length, and $L_{c,0}$ the reverse qm-corrected contour length at zero force. As a nonlinear fitting algorithm, a Levenberg−Marquardt least-squares minimization method was applied.

ASSOCIATED CONTENT

Supporting Information

The Supporting Information is available free of charge on the ACS Publications website at DOI: 10.1021/acsnano.7b02694.

Further details on experimental methods, supplementary results, and sequence information (PDF)

AUTHOR INFORMATION

Corresponding Author

*E-mail: gaub@lmu.de.

ORCID

Hermann E. Gaub: 0000-0002-4220-6088

Author Contributions

⊥W. Ott and M. A. Jobst contributed equally to this work.

Author Contributions

W.O.: experiment design, sample preparation, measurements, data analysis, writing of manuscript; M.A.J.: experiment design, data analysis, writing of manuscript; M.S.B.: data analysis; E.D.: sample preparation; L.F.M.: data analysis; M.A.N.: experiment design, writing of manuscript; H.E.G.: experiment design, writing of manuscript.

Notes

The authors declare no competing financial interest.

ACKNOWLEDGMENTS

This work was supported by the Advanced Grant "Cellufuel" of the European Research Council and the Deutsche Forschungsgemeinschaft through SFB 1032. M.A.N. acknowledges support from an ERC Starting Grant "Molecular Mechanical Adhesives" number 715207 and from Society in Science−the Branco Weiss Fellowship from ETH Zurich. We thank T. Verdorfer and C. Schoeler for proofreading and helpful discussions.

REFERENCES

(1) Cao, Y.; Li, H. Engineered Elastomeric Proteins with Dual Elasticity Can Be Controlled by a Molecular Regulator. *Nat. Nanotechnol.* **2008**, *3*, 512−516.

(2) Lv, S.; Dudek, D. M.; Cao, Y.; Balamurali, M. M.; Gosline, J.; Li, H. Designed Biomaterials to Mimic the Mechanical Properties of Muscles. *Nature* **2010**, *465*, 69−73.

(3) Rivas-Pardo, J. A.; Eckels, E. C.; Popa, I.; Kosuri, P.; Linke, W. A.; Fernández, J. M. Work Done by Titin Protein Folding Assists Muscle Contraction. *Cell Rep.* **2016**, *14*, 1339−1347.

(4) Ott, W.; Jobst, M. A.; Schoeler, C.; Gaub, H. E.; Nash, M. A. Single-Molecule Force Spectroscopy on Polyproteins and Receptor−ligand Complexes: The Current Toolbox. *J. Struct. Biol.* **2017**, *197*, 3−12.

(5) Bull, M. S.; Sullan, R. M. A.; Li, H.; Perkins, T. T. Improved Single Molecule Force Spectroscopy Using Micromachined Cantilevers. *ACS Nano* **2014**, *8*, 4984−4995.

(6) Stahl, S. W.; Nash, M. A.; Fried, D. B.; Slutzki, M.; Barak, Y.; Bayer, E. A.; Gaub, H. E. Single-Molecule Dissection of the High-

DOI: 10.1021/acsnano.7b02694
ACS Nano XXXX, XXX, XXX−XXX

Affinity Cohesin-Dockerin Complex. *Proc. Natl. Acad. Sci. U. S. A.* **2012**, *109*, 20431−20436.
(7) Schoeler, C.; Malinowska, K. H.; Bernardi, R. C.; Milles, L. F.; Jobst, M. A.; Durner, E.; Ott, W.; Fried, D. B.; Bayer, E. A.; Schulten, K.; E, G. H.; Nash, M. A. Ultrastable Cellulosome-Adhesion Complex Tightens under Load. *Nat. Commun.* **2014**, *5*, 1−8.
(8) Baumann, F.; Bauer, M. S.; Milles, L. F.; Alexandrovich, A.; Gaub, H. E.; Pippig, D. A. Monovalent Strep-Tactin for Strong and Site-Specific Tethering in Nanospectroscopy. *Nat. Nanotechnol.* **2015**, *11*, 89−94.
(9) Milles, L. F.; Bayer, E. A.; Nash, M. A.; Gaub, H. E. Mechanical Stability of a High-Affinity Toxin Anchor from the Pathogen Clostridium Perfringens. *J. Phys. Chem. B* **2017**, *121*, 3620−3625.
(10) Zimmermann, J. L.; Nicolaus, T.; Neuert, G.; Blank, K. Thiol-Based, Site-Specific and Covalent Immobilization of Biomolecules for Single-Molecule Experiments. *Nat. Protoc.* **2010**, *5*, 975−985.
(11) Zakeri, B.; Fierer, J. O.; Celik, E.; Chittock, E. C.; Schwarz-Linek, U.; Moy, V. T.; Howarth, M. Peptide Tag Forming a Rapid Covalent Bond to a Protein, through Engineering a Bacterial Adhesin. *Proc. Natl. Acad. Sci. U. S. A.* **2012**, *109*, E690−E697.
(12) Popa, I.; Rivas-Pardo, J. A.; Eckels, E. C.; Echelman, D.; Valle-Orero, J.; Fernandez, J. M. A HaloTag Anchored Ruler for Week-Long Studies of Protein Dynamics. *J. Am. Chem. Soc.* **2016**, *138*, 10546−10553.
(13) Popa, I.; Berkovich, R.; Alegre-Cebollada, J.; Badilla, C. L.; Rivas-Pardo, J. A.; Taniguchi, Y.; Kawakami, M.; Fernandez, J. M. Nanomechanics of HaloTag Tethers. *J. Am. Chem. Soc.* **2013**, *135*, 12762−12771.
(14) Pippig, D. A.; Baumann, F.; Strackharn, M.; Aschenbrenner, D.; Gaub, H. E. Protein-DNA Chimeras for Nano Assembly. *ACS Nano* **2014**, *8*, 6551−6555.
(15) Otten, M.; Ott, W.; Jobst, M. A.; Milles, L. F.; Verdorfer, T.; Pippig, D. A.; Nash, M. A.; Gaub, H. E. From Genes to Protein Mechanics on a Chip. *Nat. Methods* **2014**, *11*, 1127−1130.
(16) Oesterhelt, F.; Rief, M.; Gaub, H. E. Single Molecule Force Spectroscopy by AFM Indicates Helical Structure of Poly(ethylene-Glycol) in Water. *New J. Phys.* **1999**, *1*, 1−11.
(17) Liese, S.; Gensler, M.; Krysiak, S.; Schwarzl, R.; Achazi, A.; Paulus, B.; Hugel, T.; Rabe, J. P.; Netz, R. R. Hydration Effects Turn a Highly Stretched Polymer from an Entropic into an Energetic Spring. *ACS Nano* **2017**, *11*, 702−712.
(18) Xue, Y.; Li, X.; Li, H.; Zhang, W. Quantifying Thiol-Gold Interactions towards the Efficient Strength Control. *Nat. Commun.* **2014**, *5*, 4348.
(19) Ott, W.; Nicolaus, T.; Gaub, H. E.; Nash, M. A. Sequence-Independent Cloning and Post-Translational Modification of Repetitive Protein Polymers through Sortase and Sfp-Mediated Enzymatic Ligation. *Biomacromolecules* **2016**, *17*, 1330−1338.
(20) Tang, N. C.; Chilkoti, A. Combinatorial Codon Scrambling Enables Scalable Gene Synthesis and Amplification of Repetitive Proteins. *Nat. Mater.* **2016**, *15*, 419−424.
(21) McDaniel, J. R.; MacKay, J. A.; Quiroz, F. G.; Chilkoti, A. Recursive Directional Ligation by Plasmid Reconstruction Allows Rapid and Seamless Cloning of Oligomeric Genes. *Biomacromolecules* **2010**, *11*, 944−952.
(22) Meyer, D. E.; Chilkoti, A. Genetically Encoded Synthesis of Protein-Based Polymers with Precisely Specified Molecular Weight and Sequence by Recursive Directional Ligation: Examples from the Elastin-like Polypeptide System. *Biomacromolecules* **2002**, *3*, 357−367.
(23) Gray, W. R.; Sandberg, L. B.; Foster, J. A. Molecular Model for Elastin Structure and Function. *Nature* **1973**, *246*, 461−466.
(24) Roberts, S.; Dzuricky, M.; Chilkoti, A. Elastin-like Polypeptides as Models of Intrinsically Disordered Proteins. *FEBS Lett.* **2015**, *589*, 2477−2486.
(25) Dorr, B. M.; Ham, H. O.; An, C.; Chaikof, E. L.; Liu, D. R. Reprogramming the Specificity of Sortase Enzymes. *Proc. Natl. Acad. Sci. U. S. A.* **2014**, *111*, 13343−13348.
(26) Urry, D. W.; Hugel, T.; Seitz, M.; Gaub, H. E.; Sheiba, L.; Dea, J.; Xu, J.; Parker, T. Elastin: A Representative Ideal Protein Elastomer. *Philos. Trans. R. Soc., B* **2002**, *357*, 169−184.
(27) Valiaev, A.; Lim, D. W.; Oas, T. G.; Chilkoti, A.; Zauscher, S. Force-Induced Prolyl Cis-Trans Isomerization in Elastin-like Polypeptides. *J. Am. Chem. Soc.* **2007**, *129*, 6491−6497.
(28) Valiaev, A.; Dong, W. L.; Schmidler, S.; Clark, R. L.; Chilkoti, A.; Zauscher, S. Hydration and Conformational Mechanics of Single, End-Tethered Elastin-like Polypeptides. *J. Am. Chem. Soc.* **2008**, *130*, 10939−10946.
(29) Puchner, E. M.; Franzen, G.; Gautel, M.; Gaub, H. E. Comparing Proteins by Their Unfolding Pattern. *Biophys. J.* **2008**, *95*, 426−434.
(30) Dietz, H.; Rief, M. Exploring the Energy Landscape of GFP by Single-Molecule Mechanical Experiments. *Proc. Natl. Acad. Sci. U. S. A.* **2004**, *101*, 16192−16197.
(31) Proksch, R.; Schäffer, T. E.; Cleveland, J. P.; Callahan, R. C.; Viani, M. B. Finite Optical Spot Size and Position Corrections in Thermal Spring Constant Calibration. *Nanotechnology* **2004**, *15*, 1344−1350.
(32) Petrosyan, R. Improved Approximations for Some Polymer Extension Models. *Rheol. Acta* **2017**, *56*, 21−26.
(33) Hugel, T.; Rief, M.; Seitz, M.; Gaub, H. E.; Netz, R. R. Highly Stretched Single Polymers: Atomic-Force-Microscope Experiments versus *Ab-Initio* Theory. *Phys. Rev. Lett.* **2005**, *94*, 048301.
(34) Valiaev, A.; Lim, D. W.; Schmidler, S.; Clark, R. L.; Chilkoti, A.; Zauscher, S. Hydration and Conformational Mechanics of Single, End-Tethered Elastin-like Polypeptides. *J. Am. Chem. Soc.* **2008**, *130*, 10939−10946.
(35) Jobst, M. A.; Schoeler, C.; Malinowska, K.; Nash, M. A. Investigating Receptor-Ligand Systems of the Cellulosome with AFM-Based Single-Molecule Force Spectroscopy. *J. Visualized Exp.* **2013**, e50950.
(36) Stirnemann, G.; Giganti, D.; Fernandez, J. M.; Berne, B. J. Elasticity, Structure, and Relaxation of Extended Proteins under Force. *Proc. Natl. Acad. Sci. U. S. A.* **2013**, *110*, 3847−3852.
(37) Cheng, S.; Cetinkaya, M.; Gräter, F. How Sequence Determines Elasticity of Disordered Proteins. *Biophys. J.* **2010**, *99*, 3863−3869.
(38) Studier, F. W. Protein Production by Auto-Induction in High Density Shaking Cultures. *Protein Expression Purif.* **2005**, *41*, 207−234.
(39) MacEwan, S. R.; Hassouneh, W.; Chilkoti, A. Non-Chromatographic Purification of Recombinant Elastin-like Polypeptides and Their Fusions with Peptides and Proteins from Escherichia coli. *J. Visualized Exp.* **2014**, e51583.
(40) Anthis, N. J.; Clore, G. M. Sequence-Specific Determination of Protein and Peptide Concentrations by Absorbance at 205 Nm. *Protein Sci.* **2013**, *22*, 851−858.
(41) Gasteiger, E.; Hoogland, C.; Gattiker, A.; Duvaud, S.; Wilkins, M.; Appel, R.; Bairoch, A. Protein Identification and Analysis Tools on the ExPASy Server. *Proteomics Protocols Handbook* **2005**, 571−607.
(42) Hutter, J. L.; Bechhoefer, J. Calibration of Atomic-Force Microscope Tips. *Rev. Sci. Instrum.* **1993**, *64*, 1868−1873.
(43) Jobst, M. A.; Milles, L. F.; Schoeler, C.; Ott, W.; Fried, D. B.; Bayer, E. A.; Gaub, H. E.; Nash, M. A. Resolving Dual Binding Conformations of Cellulosome Cohesin- Dockerin Complexes Using Single-Molecule Force Spectroscopy. *eLife* **2015**.

DOI: 10.1021/acsnano.7b02694
ACS Nano XXXX, XXX, XXX−XXX